46th AIAA Aerospace Sciences Meeting and Exhibit
7 - 10 January 2008, Reno, Nevada

AIAA 2008-953

Evaluation of Chemiluminescence as a Combustion Diagnostic under Varying Operating Conditions

Venkata Nori[1] and Jerry Seitzman[2]

Ben T. Zinn Combustion Lab
Guggenheim School of Aerospace Engineering
Georgia Institute of Technology
Atlanta GA-30332-0150
U.S.A

Modeling of OH*, CH* and CO_2* chemiluminescence, using recently validated reaction mechanisms, is used to examine chemiluminescence sensing of heat release and equivalence ratio in lean, premixed methane and syngas (H_2/CO) flames. The effect of pressure, reactant preheat, aerodynamic strain, fuel-air ratio and product recirculation on spatially integrated chemiluminescence signals are considered. In the syngas mixture studied (equal molar amounts of H_2 and CO), heat release rate measurements with either OH* or CO_2* chemiluminescence are predicted to exhibit significant sensitivity to equivalence ratio (Φ), pressure, reactant temperature and (to a lesser extent) aerodynamic strain. At high pressures, the chemiluminescence is practically independent of strain rate. Mixing of hot products and reactants before burning (e.g., EGR) also has little impact. OH* chemiluminescence is found to have some advantages for heat release sensing in turbulent premixed flames at near stoichiometric conditions. It has a lower strain dependence and is less sensitive to Φ variations than CO_2* for near stoichiometric mixtures. For leaner conditions, heat release measurements employing CO_2* may be advantageous, due to its lower dependence on Φ, pressure and preheat temperature. The ratio of CO_2* to OH* chemiluminescence is not useful for equivalence ratio sensing with syngas fuels. For methane, OH*, CH* and CO_2* can be used for heat release sensing, but all are also functions of Φ, pressure and reactant preheat. OH* and CO_2* chemiluminescence are not significantly influenced by adiabatic product recirculation, while OH* and CH* are relatively insensitive to strain. Overall, CH* may be preferable for heat release sensing applications at elevated pressures and reactant temperatures such as those found in gas turbine combustors. For equivalence ratio sensing in lean methane combustion, the ratio of CH* to OH* chemiluminescence is useful, However, this ratio is highly dependent on the operating pressure and reactant temperature. For example, the ratio monotonically increases with Φ at atmospheric pressure, but monotonically decreases at high pressure. So the CH*/OH* ratio can be used for equivalence ratio sensing only at certain conditions in methane combustion. Finally thermal production of OH* in high pressure combustors, and CO_2* background for "single" wavelength detection systems can be problematic.

I. Introduction

Optical emissions from flames are widely used in combustion sensing and diagnostic applications. One source of flame emission is chemiluminescence, the electromagnetic radiation emitted from the de-excitation of electronically excited species that are formed via chemical reactions in the combustion reaction zone. Thus chemiluminescence can provide information about conditions in the reaction zone, with CH*, OH*, C_2* and CO_2* responsible for much of the visible and ultraviolet chemiluminescence in typical hydrocarbon-air flames.[1] An early experimental study in propane and ethylene fueled combustors showed that ratios of emission intensities from

[1] Graduate Research Assistant and AIAA Student Member.
[2] Associate Professor and AIAA Associate Fellow.

different species could be used to monitor fuel-air ratio.[2] Later investigations in various gaseous and liquid fuel systems have further strengthened this claim.[3-6] Chemiluminescence imaging is also routinely employed to detect flame position, shape and structure in combustors.[7,8] For combustion dynamics studies, chemiluminescence is often used as a measure of heat release fluctuations, both temporally and spatially.[9-12] However, chemiluminescence signals have to be interpreted with caution owing to their line of sight nature.[13] Additionally, the interpretation of chemiluminescence signals to infer, for example, heat release rate or equivalence ratio has been based primarily on heuristic arguments or empirical data gathered under limited conditions. For chemiluminescence sensing to be applied in practical environments, it is necessary to understand the effects of parameters such as pressure, preheat temperature, strain, equivalence ratio, exhaust gas recirculation and fuel on chemiluminescence signals. While the effect of equivalence ratio on chemiluminescence has been investigated at atmospheric conditions, for example in the studies focused on equivalence ratio sensing, there has been less effort to examine the influence of pressure[14-17] and strain[12,16] on OH* CH* and C_2* chemiluminescence, with the work limited primarily to methane flames with room temperature reactants. Since high pressure operation is often associated with preheated reactants, as in IC and gas turbine engines, an important aspect of realistic combustors has been neglected.

Chemiluminescence modeling provides an alternate and more flexible approach for understanding chemiluminescence and its dependence on various operating conditions. For example, a few studies have employed this approach to investigate the relationship between chemiluminescence and various flame properties in methane flames.[18,19] However, the accuracy of chemiluminescence simulations depends in part on the reliability of the kinetic mechanisms describing the excited state species, i.e., the reactions and rate constants for the formation and removal of the excited states. Additionally, it requires a reliable detailed chemical kinetic mechanism for the fuel-oxidizer system to accurately model the concentrations of the chemiluminescence precursor and quencher species. A number of studies have attempted to validate various OH*, CH* or C_2* chemiluminescence models through comparisons to experimental data, predominantly in methane systems.[20-23] More recently, detailed examinations of proposed OH* and CO_2* chemiluminescence mechanisms were used to identify the most reliable models for H_2/CO (syngas) and methane combustion.[22, 23] These studies compared the model predictions to experimental data for ranges of equivalence ratio, syngas fuel composition, reactant preheat temperature and CO_2 dilution at atmospheric pressure. A similar approach employing methane and Jet-A flames was used to identify a reliable model for CH* chemiluminescence.[23, 24]

The goal of the current study is to examine the dependence of OH*, CO_2* and CH* chemiluminescence on different operating conditions such as pressure, preheat, aerodynamic strain rate and reactant-product mixing (e.g., exhaust gas recirculation) for premixed combustion of methane and syngas fuels. These fuels were chosen as their combustion chemistry is well known and are highly relevant to many existing and planned ground power combustion systems, such as gas turbines. OH*, CH* and CO_2* were chosen as they occur in almost all hydrocarbon flames and because of the availability of validated mechanisms for their formation and removal. In addition, we examine the ability of flame chemiluminescence to be used for sensing important combustion parameters, specifically heat release rate and reaction zone equivalence ratio. The contribution of CO_2* background to nominal OH* and CH* signals for studies using coarse spectral resolution (e.g., photomultipliers with narrow band filters) is also considered. Additionally, the contribution of thermally produced OH* to the overall OH* signal and its importance in high pressure methane combustion is discussed.

II. Chemiluminescence Modeling

Detailed chemical kinetic calculations were performed using CHEMKIN™,[25] PREMIX[26] (for 1D, adiabatic and zero strain flames) and OPPDIFF[27] (for adiabatic, opposed and strained premixed flames). For simulating product recirculation, a reactor network was employed that combined a chemical equilibrium solver, a non-reacting gas mixer and PREMIX. Equilibrium products at a given equivalence ratio are mixed with a known mass of fresh reactants; then laminar flame calculations are carried out with the resulting mixture. GRI Mech 3.0[28] was used for both syngas and methane fuels. Multi-component and thermal diffusion were included. OH*, CH* and CO_2* intensities were evaluated from the results of the detailed chemistry simulations using post-processing algorithms. In flames, electronically excited species in general have low concentrations due to their low production rates and their rapid removal by collisional quenching. They therefore often have little impact on the overall flame chemistry. For these reasons, an excited species can often be assumed to be in quasi-steady state, with the formation rate limiting the whole process.[29,30] In this case, the excited species concentration can be determined from the ratio of its formation and removal rates. Then the photon emission rate i_c (mole photons cm^{-3} s^{-1}) from an excited state species c is given by,

$$i_c = A_c[c] \tag{1}$$

where $[c]$ is the concentration of species c and A_c is the Einstein coefficient for spontaneous emission of the electronic transition.

The computed OH*, CH* and CO_2^* photon emission profiles across the flame are integrated to produce the chemiluminescence emission per unit flame area (I_{OH^*}, I_{CH^*} and $I_{CO_2^*}$, photons $cm^{-2}\ s^{-1}$), i.e.,

$$I_c = \int_0^L i_c \, dx \tag{2}$$

where L is the integration length. Here, L is chosen such that it corresponds to a combustor residence time of 2-3 ms, which is characteristic of many practical combustors. The residence time is calculated with respect to the location in the flame where the heat release first reaches 1% of its peak value.

Table 1. Chemiluminescence reaction mechanism to model OH* and CH* formation and quenching. The spontaneous emission rate coefficients (A_c) for CH*[33] and OH*[34] are $1.85\text{x}10^6$ and $1.4\text{x}10^6\ s^{-1}$. Rate coefficients are expressed as $k = A\ T^b\ exp(-E/RT)$ in units of cal, mol, cm and s.

#	Reaction	A	b	E_a(cal)	Ref.
R1	$H + O + M \leftrightarrow OH^* + M$	$6\text{x}10^{14}$	0.0	6940	31
R3	$CH + O_2 \leftrightarrow OH^* + CO$	$3.24\text{x}10^{14}$	-0.4	4150	32
Q1	$OH^* + H_2O \rightarrow OH + H_2O$	$5.92\text{x}10^{12}$	0.5	-861	33
Q2	$OH^* + CO_2 \rightarrow OH + CO_2$	$2.75\text{x}10^{12}$	0.5	-968	33
Q3	$OH^* + CO \rightarrow OH + CO$	$3.23\text{x}10^{12}$	0.5	-787	33
Q4	$OH^* + H_2 \rightarrow OH + H_2$	$2.95\text{x}10^{12}$	0.5	-444	33
Q5	$OH^* + O_2 \rightarrow OH + O_2$	$2.10\text{x}10^{12}$	0.5	-482	33
Q6	$OH^* + OH \rightarrow OH + OH$	$1.50\text{x}10^{12}$	0.5	0.0	34
Q7	$OH^* + H \rightarrow OH + H$	$1.50\text{x}10^{12}$	0.5	0.0	34
Q8	$OH^* + O \rightarrow OH + O$	$1.50\text{x}10^{12}$	0.5	0.0	34
Q9	$OH^* + N_2 \rightarrow OH + N_2$	$1.08\text{x}10^{11}$	0.5	-1238	33
Q10	$OH^* + CH_4 \rightarrow OH + CH_4$	$3.36\text{x}10^{12}$	0.5	-635	33
R6	$C_2H + O \leftrightarrow CH^* + CO$	$6.023\text{x}10^{12}$	0.0	457	35
R7	$C_2H + O_2 \leftrightarrow CH^* + CO_2$	$6.023\text{x}10^{-4}$	4.4	-2285.1	35
Q1	$CH^* + H_2O \leftrightarrow CH + H_2O$	$5.3\text{x}10^{13}$	0.0	0.0	33
Q2	$CH^* + CO_2 \leftrightarrow CH + CO_2$	$2.41\text{x}10^{-1}$	4.3	-1694	33
Q3	$CH^* + CO \leftrightarrow CH + CO$	$2.44\text{x}10^{12}$	0.5	0.0	33
Q4	$CH^* + H_2 \leftrightarrow CH + H_2$	$1.47\text{x}10^{14}$	0.0	1361	33
Q5	$CH^* + O_2 \leftrightarrow CH + O_2$	$2.48\text{x}10^{6}$	2.14	-1720	33
Q6	$CH^* + N_2 \leftrightarrow CH + N_2$	$3.03\text{x}10^{2}$	3.4	-381	33
Q7	$CH^* + CH_4 \rightarrow CH + CH_4$	$1.73\text{x}10^{13}$	0.0	167	33

The validated reaction rate parameters for the formation and quenching reactions for OH* and CH* are given in Table 1. Unlike OH* and CH*, there is no detailed mechanism for CO_2* chemiluminescence. Rather, the validated photon emission rate $i_{CO_2^*}$ is given by a global rate that is dependent on the concentrations of [CO] and [O][36] and a rate constant for the emission intensity in the 200-700 nm spectral range for temperatures of 1300-2700 K.[37] In this

paper, we consider the CO_2* intensity at 375 nm; the rate expression at this wavelength was extracted from the spectral data reported by Slack *et al.*[37] and is given by

$$i_{CO_2^*} = 3.3(\pm 0.3) \times 10^3 \exp[-2300/T(K)][CO][O] \tag{3}$$

III. Results and Discussion

The first part of the results examines the use of chemiluminescence signals for heat release rate sensing in methane and syngas flames. The second part covers equivalence ratio sensing based on chemiluminescence signal ratios. As part of the heat release studies, the CO_2* background is estimated at the OH* and CH* detection wavelengths and its implications are discussed. Additionally, the relative contributions of thermal and chemical sources to OH* are discussed briefly.

A. Heat Release Sensing

H_2:CO=50:50 Syngas Mixture

A representative syngas mixture consisting of an equi-molar mixture of H_2 and CO is considered for this study. For H_2 and CO, the flame emission is primarily due to OH* and CO_2* chemiluminescence in the ultraviolet and visible (UV-VIS) spectrum. For examining heat release sensing, it is convenient to normalize the emission intensities with the heat release rate per unit flame area, q (W cm^{-2}), which is given by

$$q = \int_0^L q' \, dx \tag{4}$$

where q' (W cm^{-3}) is the volumetric heat release rate at a point in the flame and L again is the integration length. For sensing heat release rate, one would ideally like this normalized chemiluminescence signal to be a constant, i.e., only a weak function of other flame conditions, such as equivalence ratio, pressure and preheat temperature. In the following, the calculated normalized chemiluminescence emission intensities were scaled by a single constant to make their values convenient for plotting.

1. Effect of Pressure and Reactant Preheat

Results for normalized OH* chemiluminescence signals are shown in Figure 1(a) as a function of equivalence ratio (limited to lean operation) for different pressures and preheat conditions, with the range representative of gas turbine conditions. It has to be reiterated that the numerically computed chemiluminescence signals are representative of a residence time of 2-3 ms in the flame zone, similar to that of many practical gas turbine combustors. It is clear that the normalized OH* signal is a strong function of equivalence ratio (Φ), with as much as a five times increase from Φ=0.5 to 1 at lower pressures and almost a factor of 70 increase at 15 atm. At higher pressures, the equivalence ratio dependence changes abruptly at Φ~0.7. The reason for this rapid increase could be attributed to the rapid increase in the formation rate as compared to the quenching rate of the excited species. The quenching rate does not significantly change across the equivalence ratio considered while the formation rate increases many fold in this range. However, the flame thickness also decreases with equivalence ratio, which affects the integrated chemilumincescence intensity (I_c). Therefore, it is the complex interplay between flame thickness, OH* formation and OH* quenching that decides the magnitude of the signal. The normalized OH* chemiluminescence is seen to generally decrease with pressure for lean mixtures, except at near stoichiometric conditions. The effect of preheat on the normalized OH* signal is more uniform in that it causes an overall increase in the OH* signal throughout the equivalence ratio range. This implies that the OH* production rate, relative to the heat release, is greatly enhanced at high temperatures.

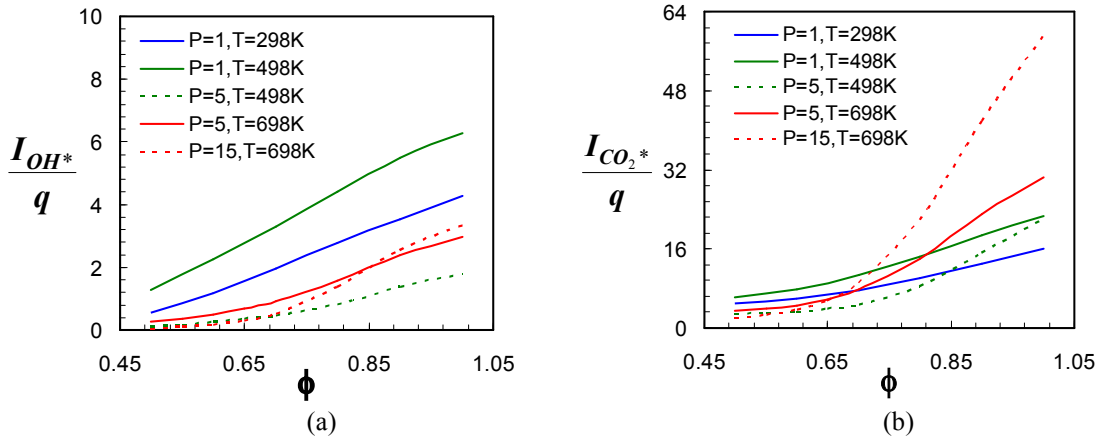

Figure 1. Variation of (a) OH*, (b) CO_2* chemiluminescence with equivalence ratio at various pressure and preheat conditions

The normalized CO_2* signal, Figure 1(b), also depends strongly on equivalence ratio but usually to a lesser degree compared to OH* chemiluminescence. It increases across the Φ=0.5-1 range by about 3.5 times at lower pressures and by ~30 times at 15 atm. However, most of this change occurs for Φ>0.7, for all the pressure and temperatures considered. Thus for very lean syngas mixtures, CO_2* chemiluminescence has some advantage for heat release rate sensing compared to OH* chemiluminescence, as minor variations in equivalence ratio and preheat temperature would cause smaller changes in the chemiluminescence signal. For example, a ±5% variation of equivalence ratio at Φ=0.6 at 15 atm and 698 K, would produce a ±18% change in the CO_2* signal per unit heat release. The same change would produce nearly twice the change (± 30%) in the OH* signal per unit heat release. The rapid increase in I_{CO2*}/q for higher equivalence ratios is attributed to the rapid increase in the formation rate of CO_2* caused by the rapid rise in temperature and [O]. It also results from significant amounts of CO_2* produced downstream of the primary reaction zone in the hot products (again when temperature and [O] are high). This would be even more important in combustors with longer residence times. In syngas flames, this also occurs for OH*, since OH* is primarily formed via the recombination of H and O atoms, which also exist in the hot product gases. However, the contribution from the post-flame zone is not as significant as for CO_2*. The pressure dependence of the normalized CO_2* signal is also different. Only at very lean equivalence ratios does the normalized CO_2* signal consistently decrease with pressure as observed for OH*. Otherwise there appears to be a non-monotonic pressure effect; an increase in pressure from 1-5 atm reduces I_{CO2*}/q, while a further increase to 15 atm produces a significant rise in the normalized signal. At a given pressure, however, the CO_2* signal per unit heat release responds like the OH* signal to a rise in reactant temperature; it increases throughout the equivalence ratio range.

2. Effect of Aerodynamic Strain Rate

The analysis above is based on simulations of unstrained laminar flames. Practical combustors, on the other hand, rely on turbulent flames to produce high volumetric efficiencies. One characteristic of turbulent flames is the aerodynamic strain produced. Aerodynamic strain affects the diffusion rates of species and temperature, and modifies the residence times of the various species in the flame front, which indirectly has an effect on the reaction kinetics. Therefore, it is useful to examine the effects of aerodynamic strain rate on flame chemiluminescence. A framework for numerical modeling of chemiluminescence in opposed flow, laminar strained flames has been previously demonstrated.[29] This approach is employed here, with the OH* and CO_2* signals again normalized by the heat release rate per unit flame area. However, in this case, the volumetric heat release rate (q') profile is integrated up to the stagnation plane.

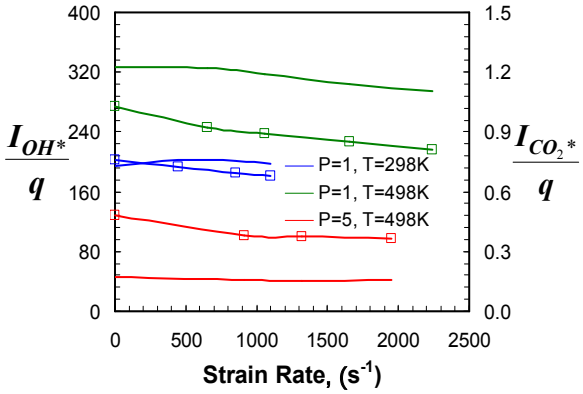

Figure 2. Strain rate dependence of OH* (solid lines) and CO_2* (symbols on lines) chemiluminescence in H_2:CO=50:50 syngas mixture.

Results for OH* and CO_2* chemiluminescence with varying strain rate, at different pressure and preheat conditions, are given in Figure 2. The equivalence ratio of the mixture is fixed at 0.7. The zero strain solution corresponds to that of the one-dimensional laminar premixed flame. The CO_2* signal per unit heat release continuously decreases with strain for the atmospheric pressure cases. However for the higher pressure case, the CO_2* signal is essentially independent of strain, except for an initial drop from the zero strain solution. This drop may be due to the difference in the calculation approaches for the zero strain and strained flames rather than being indicative of a strain effect. Preheat does not seem to effect the behavior of the normalized CO_2* signal with strain (other than to increase I_{CO2*}/q as noted previously). Since q decreases with strain, the results show that the CO_2* signal decreases faster than q with strain. The normalized OH* signal (Figure 2) also decreases continuously with strain, except for the ambient temperature and pressure case. I_{OH*}/q is less sensitive to strain, decreasing by 11% at most for the conditions examined, whereas I_{CO2*}/q changes by 30%. Thus the results also suggest that the chemiluminescence ratio I_{CO2*}/ I_{OH*} will also decreases with strain.

Summarizing the findings up to this point, OH* chemiluminescence can be identified as a better heat release marker for turbulent premixed syngas flames at near stoichiometric conditions. It has a lower strain dependence and is less sensitive to equivalence ratio variations for these conditions. For leaner conditions, heat release measurements employing CO_2* may be advantageous, due to the lower dependence on changes in Φ and preheat temperature, even though the strain dependence is somewhat greater.

3. Effect of Reactant Product Mixing

The influence of hot products mixing with reactants before combustion occurs is another aspect of practical combustors that needs to be considered. Exhaust gas recirculation (EGR) is a popular strategy for NOx control in many practical combustion devices.[38-40] In addition, reactant-product mixing can also occur as part of the stabilization processes in combustors. For example in gas turbine combustors, the swirl stabilization produces zones in the combustor where product recirculation occurs. Therefore, we examine the effect of product recirculation on flame chemiluminescence. The fraction of product gas in the reactants is commonly quantified by an EGR ratio, specifically the mass ratio of recycled gases to the total mass of the mixture.

Adiabatic product recirculation (also called hot EGR) was examined for a syngas equivalence ratio of 0.7, and for EGR ratios of 5, 11 and 20%, and a range of pressures and preheat conditions. Note, the final product temperature is independent of EGR since adiabatic product recirculation is simulated. Results are shown for the normalized OH* and CO_2* chemiluminescence in Figure 3. Neither I_{OH*}/q nor I_{CO2*}/q is appreciably affected by product recirculation. The normalized OH* signal does increase somewhat with recirculation (by ~10%) at atmospheric pressure. For example at 11% EGR, I_{OH*}/q increases by about 6% at 298 K and 9% at 498 K compared to the 0% EGR case. The effect at higher pressure is even smaller, I_{OH*}/q is practically constant at 5 atm. The CO_2* signal (I_{CO2*}/q) varies only slightly (a few percent), increasing at 1 atm and decreasing at 5 atm. Reactant preheating does not change this result. In summary, product recirculation does not appear to significantly impact the ability of OH* or CO_2* chemiluminescence to provide measurements of heat release in syngas fuels. The results also suggest that product recirculation would have little effect on the ratio I_{CO2*}/ I_{OH*}.

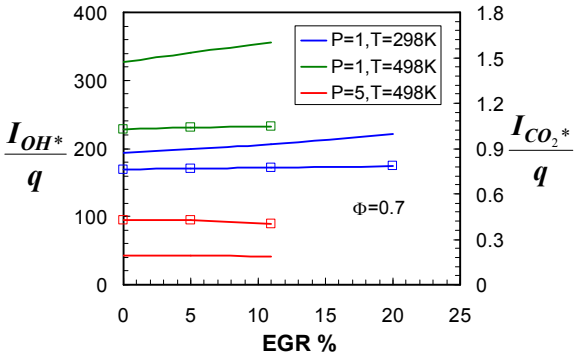

Figure 3. Dependence of OH* (solid lines) and CO_2* (symbols on lines) chemiluminescence on product recirculation in a H_2:CO=50:50 syngas mixture.

Methane

In methane-air premixed flames, there are three chemiluminescence emitters in the UV-VIS: OH*, CH* and CO_2*. However in practical combustors, the CO_2* signal can be corrupted with emissions from other molecules, such as HCO, and interferences from blackbody radiation sources, e.g., soot and combustor walls.

1. Effect of Pressure and Reactant Preheat

Results for OH* chemiluminescence are presented in Figure 4. As in the syngas case, the normalized OH* signal is a strong function of equivalence ratio. I_{OH*}/q increases by six times at atmospheric pressure for $0.6<\Phi<1$. At high pressure (15 atm), the dependence is even greater, with an increase of 20 times for the same Φ range. Pressure in general, decreases the normalized OH* signal over the entire Φ range. However, this decrease is more pronounced

for leaner mixtures. This effect has also been observed in an earlier experimental study.[15] At a given equivalence ratio and pressure, preheating also increases the normalized OH* signal, and again the increase is more pronounced for leaner conditions. Overall, the variation with pressure over typical operating conditions is more significant than the preheating effect.

These results can be explained by examining the OH* formation and destruction rates. OH* is formed from reactions R1 and R3 (shown in Table 1). R3 is relevant in the reaction zone where CH is found, whereas R1 occurs in both the primary reaction zone and in the product gases where O and H atoms are still found. Moreover, R1 is more pressure dependent. R3 dominates the overall formation in low pressure environments, responsible for almost 90% of the OH* signal at atmospheric pressure. However at 15 atm, R1 contributes roughly 50% of the total OH* production. As R3 primarily occurs in the primary reaction zone, the integrated OH* signal decreases as the pressure increases and the flame thickness decreases, even though the formation rate increases manyfold. This, compounded with the increased q at elevated pressures, results in a lower normalized OH* signal. It should also be noted that at elevated pressures, dissociation is inhibited. This and lower temperatures for leaner equivalence ratios reduces mole fractions of the radicals (CH, O and H) necessary for OH* formation.

The dependence of OH* chemiluminescence-based heat release sensing to equivalence ratio fluctuations can be determined from Figure 4. In general, there is less dependence at near stoichiometric conditions. For example at 15 atm, a ±5% equivalence ratio fluctuation around a mean value of Φ=0.9 would cause a ±20% change in the sensitivity of chemiluminescence to heat release rate. The same ±5% fluctuation at Φ=0.55, would cause a larger (±30%) change. Similarly for reactant preheat and pressure fluctuations, the relation between OH* chemiluminescence and heat release shows less variation at near stoichiometric conditions. For example at 5 atm and a 200 K preheat change, I_{OH*}/q increases by 35% at Φ=1.0 whereas it increases by twice that (70%) at Φ=0.7.

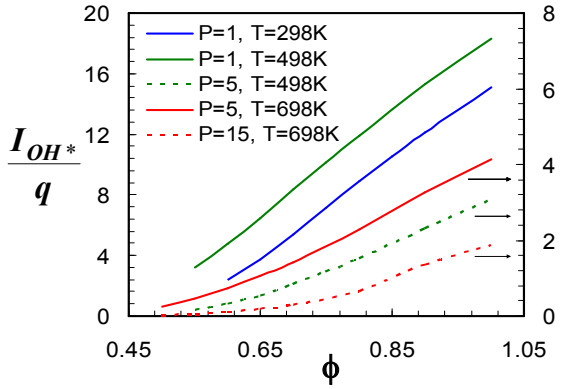

Figure 4. OH* chemiluminescence in methane at various pressure and preheat; the high pressure results are scaled to the right axis.

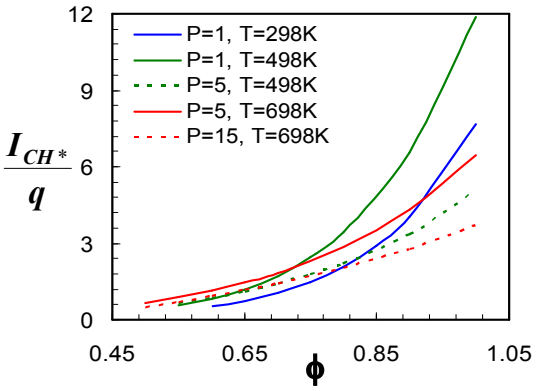

Figure 5. CH* chemiluminescence in methane at various pressure and preheat conditions.

The results for CH* chemiluminescence are shown in Figure 5. The normalized CH* signal increases by as much as 15 times at atmospheric conditions but only by four times at 15 atm for 0.6<Φ<1. Thus in contrast to OH* chemiluminescence, the equivalence ratio dependence is reduced for CH* at high pressure. Like OH*, reactant reheating increases I_{CH*}/q, by 1.5 times at atmospheric pressure, uniformly throughout the equivalence ratio range. However at 5 atm, a 200 K preheat enhances I_{CH*}/q more for leaner mixtures. Also for a given temperature and equivalence ratio, pressure decreases I_{CH*}/q, with the decrease more pronounced near Φ=1.0. For example raising the pressure from 5 to 15 atm results in a drop in I_{CH*}/q of 43% at Φ=1.0, but only 20% at Φ=0.6. Similar trends were observed in an earlier experimental effort.[16]

To compare CH* to OH* for heat release sensing, we examine the dependence of I_{CH*}/q to fluctuations in equivalence ratio and reactant temperature. For equivalence ratio oscillations at 15 atm, a ±5% change in equivalence ratio produces a ±15% change in I_{CH*}/q. However at 15 atm, similar fractional changes in equivalence ratio would produce a ±20% fluctuation at Φ=0.9 and a ±30% change at Φ=0.55, in OH* signal. This suggests that CH* is better suited for high pressure applications of heat release sensing compared to OH*. In addition, preheating

has a weaker effect on I_{CH*}/q compared to I_{OH*}/q.

CO_2* results are given in Figure 6. The normalized CO_2* signal also increases with equivalence ratio, with a dramatic increase at elevated pressure and preheat conditions. As before, preheating also increases I_{CO_2*}/q, but the increase is more pronounced at near stoichiometric and high pressure conditions. The normalized CO_2* signal also decreases when the pressure is increased from 1 to 5 atm, e.g., 28% at Φ=1.0 and 60% at Φ=0.6. At higher pressures (15 atm), the signal initially decreases for 0.5<Φ<0.8 and then increases drastically to Φ=1.0. This increase in the CO_2* background at high pressures in laminar premixed methane-air flames has been observed experimentally.[14] CO_2* intensity is directly proportional to the product of CO and O, therefore the CO_2* profile peaks in the reaction zone, but recombination of CO and O in the product gases continues to produce CO_2* in post-flame region. The contribution of the post-flame CO_2* increases dramatically near stoichiometric conditions, to the extent that it can contribute at least half the total signal if the product gases are given sufficient residence time. Since the post-flame region has negligible heat release, I_{CO_2*}/q increases. At lower equivalence ratios, the cooler post-flame gases produce little CO_2* (in addition, the reaction zone CO_2* also decreases due to lower [O] concentrations). So like OH*, but unlike CH*, the CO_2* chemiluminescence can strongly depend on combustor residence time – or at least the residence time covered by the detection optics.

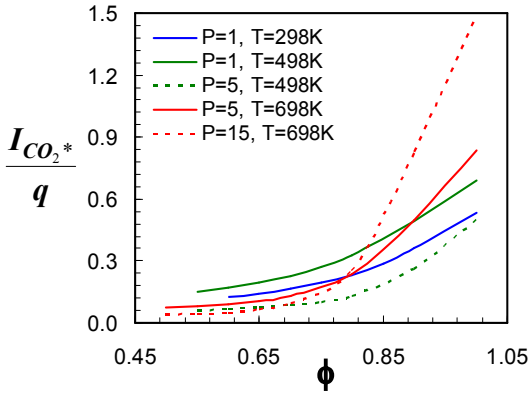

Figure 6. CO_2* chemiluminescence in methane at various pressures and preheat conditions

At atmospheric pressure, CO_2* heat release sensing shows the least sensitivity to equivalence ratio fluctuations. For example, a 5% change in Φ produces a ±17% and ±10% change in I_{CO_2*}/q at Φ=0.9 and 0.6, respectively. However at elevated pressure, I_{CO_2*}/q is very sensitive to equivalence ratio fluctuations near stoichiometric conditions. At 15 atm, a 5% change in Φ results in a I_{CO_2*}/q change of ±40% (Φ=0.9) and ±20% (Φ=0.6). So at high pressures, CO_2* is suitable as a heat release marker only under very lean equivalence ratios (Φ<0.65). Preheating at atmospheric pressure increases I_{CO_2*}/q uniformly by ~28%, but at 5 atm, with the same 200 K increase, the I_{CO_2*}/q rises by 65% at Φ=1.0 and 35% at Φ=0.6. So for Φ<0.65, both pressure and temperature fluctuations would have a reduced impact on heat release sensing with CO_2* chemiluminescence.

2. Effect of Aerodynamic Strain Rate

Results are shown for the normalized OH* and CH* signals in Figure 7 for an equivalence ratio of 0.7. I_{CH*}/q is somewhat more dependent on strain at atmospheric conditions than I_{OH*}/q. Reactant preheating makes both signals less dependent on strain. For the high pressure case, both signals are practically independent of strain. This may be because both preheat and pressure result in thinner flames, which require higher strain rates to influence the reaction zone. Similar trends were observed for calculations for an equivalence ratio of 1.0.

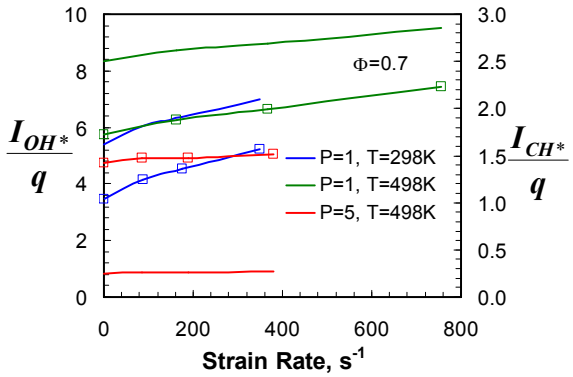

Figure 7. Strain rate dependence of OH* (solid lines) and CH* (lines with symbols) chemiluminescence in methane-air flames.

CO_2* results, though not shown here, show interesting trends. The normalized CO_2* signal decreases with strain rate for all conditions. This is because as strain rate increases, the residence time decreases, which reduces the CO_2* signal. As discussed earlier, this residence time effect is more prominent in near stoichiometric flames. So under stoichiometric conditions, the normalized CO_2* signal decreases by as much as 50% compared to the unstrained case, even at high pressure. Thus CO_2* should be avoided for heat release sensing in strained flames except at very lean equivalence ratios.

3. Effect of Reactant Product Mixing

Results for OH* and CH* with adiabatic product recirculation are shown in Figure 8 at an equivalence ratio of 0.7. As in the syngas case, the normalized OH* signal is practically unaffected by product recirculation at the pressure and preheat conditions studied here. CO_2* results, again not shown, closely resemble the OH* data. On the other hand, the normalized CH* signal is significantly affected by product recirculation. It increases by as much as 50% for the 20% EGR case.. In these cases, q increases with EGR. This implies that I_{CH*} increases faster than q.

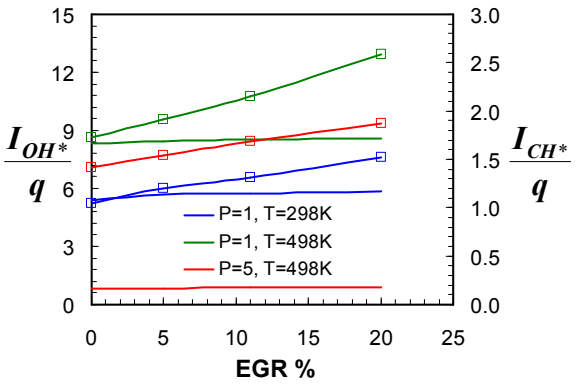

Figure 8. Dependence of OH*(solid lines) and CH*(lines with symbols) chemiluminescence on product recirculation in methane-air flames.

B. Equivalence Ratio Sensing

H_2:CO=50:50 Syngas Mixture

As previously noted, chemiluminescence intensity ratios have been used to sense equivalence ratio in various combustion systems. In syngas flames, only ratio, i.e. CO_2*/OH* ratio can be measured. The computed emission ratios for our syngas mixture were scaled by a constant to match experimental data at atmospheric conditions in a previous study.[22, 23] The simulated chemiluminescence ratios obtained at different conditions are scaled by the same constant multiplier used in the baseline atmospheric case for meaningful comparison.

1. Pressure and Reactant Preheat

It was already observed in atmospheric studies that the CO_2*/OH* signal ratio is not very useful for equivalence ratio sensing except at very lean conditions.[23] The elevated pressure and temperature results are compared with the baseline atmospheric case. It can be seen from Figure 9 that the variation of I_{CO_2*}/I_{OH*} with Φ at elevated pressures and temperatures is not appreciably different from the baseline case. Experimental data from a previous work at atmospheric conditions are also shown for convenience.[23] Pressure increases the magnitude of I_{CO_2*}/I_{OH*} throughout the equivalence ratio range, as suggested by the data shown in Figure 1. Similarly, preheating at a given pressure causes a decrease in the ratio. This may be due to the greater temperature dependence of OH* formation compared to the CO_2*. Nevertheless, I_{CO_2*}/I_{OH*} would make a poor choice for sensing equivalence ratio in the range of pressures and temperatures considered.

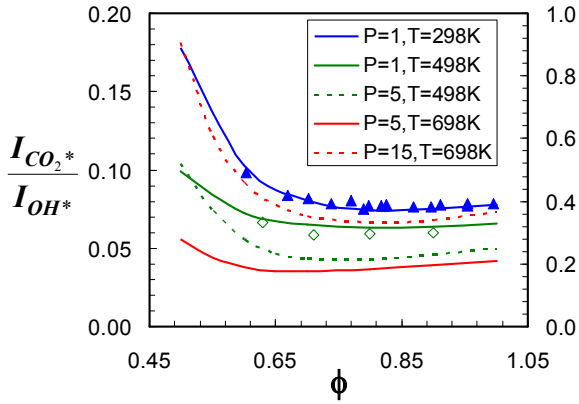

Figure 9. Variation of the CO_2*/OH* chemiluminescence ratio with equivalence ratio at various pressure and preheat conditions. The atmospheric data (symbols) is scaled with the left axis; the rest of the data scale with the right axis.

Methane

In methane premixed flames, I_{CH*}/I_{OH*} has been shown to be a promising candidate for sensing equivalence ratio at various pressures.[16] I_{CO_2*}/I_{OH*} was also investigated at atmospheric conditions, and it was found to be non-monotonic and only weakly sensitive to Φ.[23] So, it is not considered further here. Again, the computed I_{CH*}/I_{OH*} values were scaled by a constant to match experimental data acquired in a swirl combustor, at atmospheric conditions, in an earlier study.[23] The simulated chemiluminescence ratios obtained at different conditions are scaled by the same constant multiplier used for matching the modeling results with the baseline atmospheric experimental results, for meaningful comparison.

1. Pressure and Reactant Preheat

The CH* to OH* chemiluminescence ratio results are shown in Figure 10. At atmospheric pressure, I_{CH*}/I_{OH*} monotonically increases as expected. At 5 atm, there is little change in I_{CH*}/I_{OH*} with equivalence ratio, except for very lean conditions, i.e., Φ<0.65. This suggests that I_{CH*}/I_{OH*} cannot be used for sensing equivalence ratio in

some conditions. At even higher pressures (15 atm), I_{CH^*}/I_{OH^*} again varies significantly with Φ, now decreasing monotonically. At a given equivalence ratio, pressure generally increases the magnitude of the ratio. So, I_{CH^*}/I_{OH^*} can be used for sensing equivalence ratio only at certain conditions, and the changing relationship between I_{CH^*}/I_{OH^*} and Φ with pressure must be taken into account. Such trends are already reported experimentally and the effect of pressure and equivalence ratio on CH* to OH* ratio have been systematically investigated at room temperature conditions.[16]

2. Effect of Aerodynamic Strain Rate

Results for I_{CH^*}/I_{OH^*} variations with strain rate are given in Figure 11 at Φ=0.7 and 1. It was noted above that CH* chemiluminescence is more dependent on strain than OH*. This is clearly evident here, where CH*/OH* ratio increases with strain rate. For a given strain rate, the increase in I_{CH^*}/I_{OH^*} is almost the same for both equivalence ratios considered, except at high pressure. The maximum increase of 13% occurs at ambient pressure conditions, while for the higher pressure and preheat case, the I_{CH^*}/I_{OH^*} ratio increases by 1% for the lean case and increases by about 10% for the stoichiometric case. However, with I_{CH^*}/I_{OH^*} varying by only 10% over a wide range of strain rates, it can be concluded that I_{CH^*}/I_{OH^*} is not very sensitive to strain rate. This is supported by the agreement between results in laminar and turbulent combustors at atmospheric conditions.[4]

3. Effect of Reactant Product Mixing

Results for I_{CH^*}/I_{OH^*} variations with product recirculation are shown in Figure 12 for two equivalence ratios: Φ=0.7 and 1. It was seen in an earlier section that the CH* signal increases with product recirculation while OH* signal is practically unaffected by it. So as expected, I_{CH^*}/I_{OH^*} increases with product recirculation. For Φ=0.7 and 20% EGR, I_{CH^*}/I_{OH^*} increases by 27% at 5 atm and 498 K, while at 1 atm and for both 298 and 498 K reactant temperatures, the ratio increases more. Similar results are observed for the stoichiometric case. However, for lower levels of product mixing (EGR<5%), the effect on I_{CH^*}/I_{OH^*} is negligible.

C. Other Considerations

Thermal Excitation

In addition to chemical formation of the excited states, thermal excitation can also occur. Thermal OH* shall be considered as an example, and the contribution of thermal OH* emission to the total signal is examined. Similar analysis can be performed for CH*. The contribution of OH* emission due to thermally excited ground state OH molecules will increase with temperature. The procedure for calculating the upper estimate of thermal OH* based on equilibrium calculations is outlined elsewhere.[22] This methodology along with the assumption that the formation

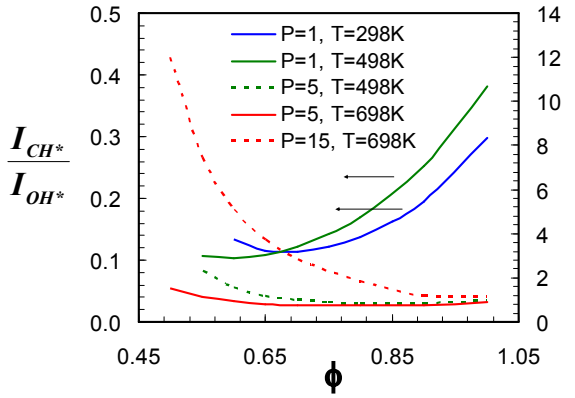

Figure 10. CH*/OH* chemiluminescence ratio in methane-air flames at various pressures and preheat; the high pressure results are scaled to the right axis.

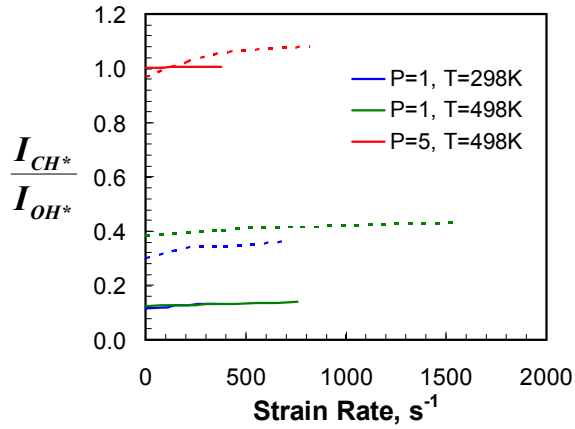

Figure 11. Dependence of CH*/OH* ratio with strain rate for Φ =1(dashed line) and Φ =0.7(solid line)

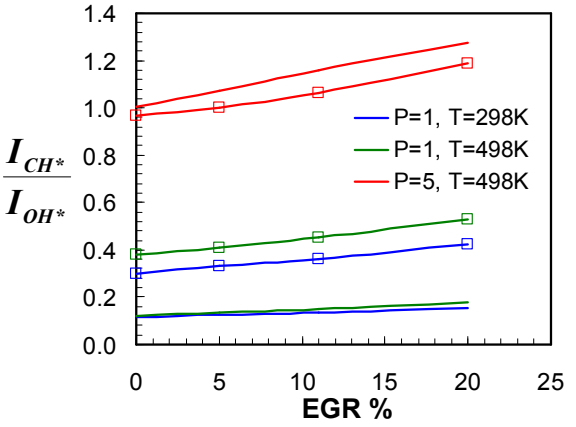

Figure 12. Dependence of CH*/OH* chemiluminescence ratio with product recirculation at Φ=0.7 (solid lines), Φ=1.0 (lines with symbols).

reactions are accurate in predicting the absolute concentrations of OH* is used to estimate thermal OH* in methane flames. Results for thermal OH* as a fraction of the total OH* for premixed methane flames are presented in Table 2. It can be clearly seen that thermal OH* is a function of residence time and the equivalence ratio of the combustor (as thermal OH* is formed primarily in the hottest regions). However, the thermal contribution to the total OH* signal also rises significantly with pressure. (As described in a previous section, the chemical formation of OH* decreases at high pressures). Hence in high pressure combustors, especially combustors with long residence times and near stoichiometric conditions, the OH* emission has to be treated carefully.

Table 2. Thermal OH* contribution (as percentage of the total OH* signal) in methane flames.

Pressure and Temperature	% Thermal OH for 2-3 ms		% Thermal OH for10 ms	
	Φ = 0.7	Φ = 1.0	Φ = 0.7	Φ = 1.0
1 atm, 298 K	0.015	0.41	0.031	1.2
1 atm, 498 K	0.063	0.76	0.28	4.4
5 atm, 498 K	0.67	8.0	2.3	20.7
5 atm, 698 K	2.25	12.8	5.1	26.5
15 atm, 698 K	12.5	33.4	29.6	40.9

CO_2 Background

Most of the time flame chemiluminescence is acquired using interference filters and detectors such as photomultiplier tubes, photodiodes or CCD cameras. The interference filters usually have a bandpass of ±5-10 nm about the center wavelength. It is also well known that CO_2* background is present in the 200-600 nm region.[29, 37] Thus, it underlies the other (OH* and CH*) emission signals. So unless a spectrometer or additional detector is used to monitor the CO_2* background, it can not be removed from the total signal. Thus it is interesting to estimate the contribution of the CO_2* background to the total signal at OH* and CH* wavelengths. Resolved flame spectra are available for swirl-stabilized methane flames at atmospheric conditions,[23] which can be reanalyzed to study the CO_2* background. The OH^* signal, S_{OH^*}, was found by integrating the (0,0) band over a 5 nm bandwidth centered at the OH^* peak (~309 nm). The CH^* signal, S_{CH^*}, was found by integrating the 430 nm CH band over a bandwidth of 5 nm. The CO_2* background over the same 5 nm bandwidth at OH* and CH* bandheads was approximated by the means of a cubic polynomial. The area under this polynomial was taken as the estimate for the CO_2* background. Results for methane are shown in Figure 13. It can be clearly seen that CO_2* background affects the CH* signal more than the OH* signal. For example at Φ=0.8, only 30% of the total signal at the CH* wavelength is from CH* chemiluminescence, while OH* chemiluminescence makes up 80% of its total signal. Moreover, the CO_2* background has a weaker equivalence ratio dependence for the OH* signal than for the CH* signal. So, CH* and OH* signals should be interpreted by accounting for the CO_2* background contribution.

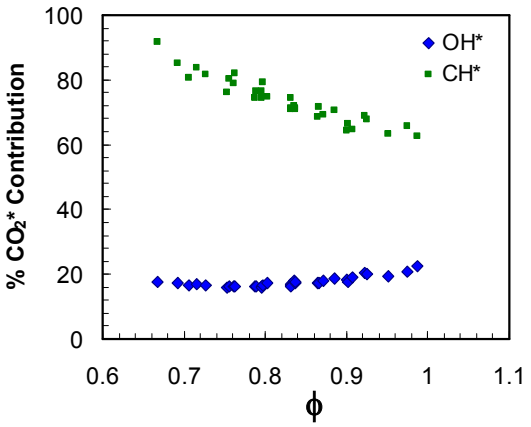

Figure 13. CO_2* contribution in methane-air flame at OH*(309±5 nm) and CH* (431±5 nm) signals.

IV. Conclusions

The effects of important combustor parameters on flame chemiluminescence have been systematically investigated in a representative syngas fuel (H_2: CO=50:50) and methane. OH* and CO_2* are the principal emitters in syngas flames, while in lean methane flames, CH* also plays an important role. Flame chemiluminescence from OH*, CH* and CO_2* were modeled using well validated reaction mechanisms describing the formation and destruction rates for the chemiluminescence species along with GRI Mech 3.0. For investigating heat release sensing, the chemiluminescence signals were normalized with spatially integrated, heat release rate per unit flame area. In the syngas mixture, pressure decreases the normalized OH* chemiluminescence, with a larger impact for leaner equivalence ratios. This is primarily due to the fact that pressure inhibits dissociation, and the lower

temperatures at very lean conditions deprive the radical precursors such as O, H, thereby affecting the OH* formation. However, the pressure effect on CO_2* is non-uniform and non-monotonic. For leaner mixtures, the normalized CO_2* signal decreases with pressure. On the other hand, it increases quite rapidly at near stoichiometric conditions. Both the normalized signals vary significantly with equivalence ratio, which implies that none of them are ideal for heat release sensing. Reactant preheating increases the magnitude of the signals throughout the equivalence ratio range. Aerodynamic strain rate tends to have a decreasing effect on both the signals, with the CO_2* signal more sensitive to strain rate than OH*. The normalized OH* signal decreased by 11% for most of the cases, whereas normalized CO_2* changed by 30%. However, the strain sensitivity decreases greatly at higher pressures. The simulated results indicate that product recirculation does not have any significant effect on either OH* or CO_2* chemiluminescence signals. With respect to heat release rate sensing in syngas fuels, CO_2* appears to be a better option at very lean equivalence ratio conditions ($\Phi < 0.7$), as it has the least sensitivity to equivalence ratio, pressure and temperature changes. Even strain rate and product recirculation would not affect CO_2*. The chemiluminescence intensity ratio CO_2*/OH* was also investigated for equivalence ratio sensing applications in syngas combustion. The CO_2*/OH* ratio is a strong function of pressure, increasing monotonically. Reactant preheating tends to decrease the ratio for all lean mixtures, but with less impact than pressure. However, the ratio remains essentially constant for $0.7<\Phi<1.0$, limiting its usefulness for equivalence ratio sensing. The ratio does monotonically increases for very lean conditions ($\Phi<0.7$) consistently over a wide range of pressure and preheat conditions. For combustors that operate under such lean conditions, the CO_2*/OH* ratio can potentially be used for sensing equivalence ratios in syngas combustion.

In methane flames, pressure has a very strong effect on the normalized OH* signal; it decreases with pressure, with the decrease more pronounced for leaner mixtures. Pressure also decreases the normalized CH* signal, but more for near stoichiometric conditions. For the normalized OH* signal, reactant preheating significantly affects leaner mixtures. Both normalized OH* and CH* signals increase with strain rate, with the increase more significant in the case of CH* at atmospheric conditions. However, both pressure and preheat tend to decrease the sensitivity to strain rate. The normalized CO_2* signal decreases with strain rate for all pressure and preheat conditions and this decrease is more prominent at near stoichiometric conditions. This is because of the reduced residence time due to flame straining. So, CO_2* should be avoided for heat release sensing in strained flames except at very lean equivalence ratios. Product recirculation has practically no effect on the normalized OH*and CO_2* signals, under the pressure and preheat conditions studied. However, the normalized CH* is affected and increases by as much as 50% for a 20% EGR at an equivalence ratio of 0.7. Compared to OH* and CO_2*, CH* would be more advantageous to use as a heat release marker at high pressure and high temperature conditions as it has the least sensitivity to fluctuations in equivalence ratio, pressure, preheat and strain rate. However, CH* data should be interpreted with caution in systems with large product recirculation. The intensity ratio CH*/OH* ratio was investigated for equivalence ratio applications. Pressure has a strong increasing effect on the CH*/OH* ratio, while the effect of preheat is not systematic. At atmospheric conditions, the ratio tends to monotonically increase with equivalence ratio, while at high pressures, the ratio monotonically decreases with pressure. However, at intermediate pressures the ratio tends to saturate and it changes very little across the equivalence ratio range. So, CH*/OH* ratio can be used for equivalence ratio sensing only at certain conditions in methane combustion.

The contribution of thermally produced OH* to the overall OH* signal was also calculated based on equilibrium conditions for methane systems. It was found that thermal pathway is not very significant at atmospheric and intermediate pressures, but it becomes increasingly important at high pressure systems. For example at 15 atm, the contribution of thermally produced OH* to the total signal could be as much as 30% for stoichiometric methane combustion with short residence times. The thermal pathway being strongly encouraged by high temperatures, it rapidly increases as near stoichiometric conditions are approached. Additionally, it also increases with combustor residence time. Therefore, OH* signal should be carefully interpreted in high pressure systems with long residence times.

The contribution of CO_2* background to the total signal at OH* and CH* wavelengths has been studied at atmospheric conditions for methane. It was observed that the CO_2* background made up only a small fraction (~20%) of the total OH* signal, but can contribute ~70% of the nominal CH* signal. The CO_2* background contribution for the OH* signal did not vary with equivalence ratio whereas it strongly varies for the CH* signal.

Acknowledgments

This research was supported by NASA through the University Research, Engineering, and Technology Institute for Aeropropulsion and Power, under Grant/Cooperative Agreement Number NCC3-982.

References

[1] Gaydon, A. G., and Wolfhard, H. G., *Flames: Their Structure, Radiation, and Temperature*. Fourth edition, Chapman and Hall, 1978.

[2] Clark, T., "Studies of OH, CH, CO and C_2 Radiation from Laminar and Turbulent Propane-Air and Ethylene-Air Flames," NACA-TN-4266, 1958.

[3] Docquier, N., Lacas, F., and Candel, S., "Closed-loop Equivalence Ratio Control of Premixed Combustion using Spectrally Resolved Chemiluminescence Measurements," *Proceedings of the Combustion Institute* **29**, 2002, pp 139-145.

[4] Muruganandam, T. M., Kim, B. H., Morrell, M, R., Nori, V., Patel, M., Romig, B. W., and Seitzman, J. M., "Optical Equivalence Ratio Sensors for Gas Turbine Combustors," *Proceedings of the Combustion Institute* **30**, 2005, pp. 1601-1609.

[5] Yamazaki, M., Ohya, M., and Tsuchiya, K. *Int. Chem. Eng.* **30**, 1992, pp. 160–168.

[6] Kojima, J., Ikeda, Y., and Nakajima, T., "Spatially Resolved Measurement of OH*, CH* and C_2* Chemiluminescence in the Reaction Zone of Laminar Methane/Air Premixed Flames," *Proceedings of the Combustion Institute* **28**, 2000, pp. 1757-1764.

[7] Stojkovic, B. D., Fansler, T. D., Drake, M. C., and Sick, V., "High-speed Imaging of OH* and Soot Temperature and Concentration in a Stratified-Charge Direct-Injection Gasoline Engine," *Proceedings of the Combustion Institute* **30**, 2005, 2657-2665.

[8] Schefer, R. W., "Flame Sheet Imaging using CH Chemiluminescence," *Combustion Science and Technology* **126** (1-6), 1997, pp. 255-270.

[9] Lee, J. G., Kim, K., and Santavicca, D. A., "Measurement of Equivalence Ratio Fluctuation and Its Effect in Heat Release During Unstable Combustion," *Proceedings of the Combustion Institute* **28**, 2000, pp. 415–421.

[10] Bellows, B. D., Zhang, Q., Neumeier, Y., Lieuwen, T., and Zinn, B. T., "Forced Response Studies of a Premixed Flame to Flow Disturbances in a Gas Turbine Combustor," AIAA Paper 2005-1164, Jan. 2005.

[11] Balachandran, R., Ayoola, B. O., Kaminski, C. F., Dowling, A. P., and Mastorakos, E., "Experimental Investigation of the Nonlinear Response of Turbulent Premixed Flames to Imposed Inlet Velocity Oscillations," *Combustion and Flame* **143** (1-2), 2005, pp. 37-55.

[12] Hardalupas, Y., and Orain, M., "Local Measurements of the Time-Dependent Heat Release Rate and Equivalence Ratio using Chemiluminescent Emission from a Flame," *Combustion and Flame* **139**, 2004, pp.188-207.

[13] Najm, H. N., Paul, P. H., Mueller, C. J., and Wyckoff, P. S., *Combustion and Flame* **113** (3), 1998, pp. 312-332.

[14] Ikeda, Y., Kojima, J., and Hashimoto, H., "Local Chemiluminescence Spectra Measurements in a High Pressure Laminar Methane/Air Premixed Flame," *Proceedings of the Combustion Institute* **29**, 2002, pp.1495-1501.

[15] Higgins, B., McQuay, M. Q., Lacas, F., Rolon, J. C., Darabiha, N., and Candel, S., "Systematic Measurements of OH Chemiluminescence for Fuel-Lean, High-Pressure, Premixed, Laminar Flames," *Fuel* **80**(1), 2001, pp. 67-74.

[16] Higgins, B., McQuay, M. Q., Lacas, F., and Candel, S., "An Experimental Study on the Effect of Pressure and Strain Rate on CH Chemiluminescence of Premixed Fuel-Lean Methane/Air Flames," *Fuel* **80**(11), 2001, pp. 1583-1591.

[17] Docquier, N., Belhafaoui, S., Lacas, F., Darabiha., and Rolon, J-C., "Experimental and Numerical Study of Chemiluminescence in Methane/Air High-Pressure Flames for Active Control Applications," *Proceedings of the Combustion Institute* **28**, 2000, pp. 1765-1774.

[18] Kojima, J., Ikeda, Y., and Nakajima, T., "Basic Aspects of OH(A), CH(A), and C_2(d) Chemiluminescence in the Reaction Zone of Laminar Methane-Air Premixed Flames," *Combustion and Flame* **140**, 2005, pp. 34-45.

[19] Haber, L. C., Vandsburger, U., Saunders, W, R., and Khanna, V. K., *Proceedings of International Gas Turbine Institute*, 2000.

[20] Walsh, K. T., Long, M. B., Tanoff, M. D., and Smooke, M. D., "Experimental and Computational Study of CH, CH*, and OH* in an Axisymmetric Laminar Diffusion Flame," *Proceedings of the Combustion Institute* **27**, 1998, pp. 615-623.

[21] Leo, Maurizio De., Saveliev, A., Kennedy, L. A., and Zelepouga, S. A., "OH and CH Chemiluminescence in Opposed Flow Methane Oxy-Flames," *Combustion and Flame* **149**, 2007, pp. 435-447.

[22] Nori. V. N., and Seitzman, J. M., "Models for OH* and CO_2* Chemiluminescence Sensing in Flames," submitted to *Combustion and Flame*.

[23] Nori, V. N., and Seitzman, J. M., "Chemiluminescence Measurements and Modeling in Syngas, Methane and Jet-A Fueled Combustors," AIAA-2007-466, 45th AIAA Aerospace Sciences Meeting and Exhibit, Reno, Nevada, Jan. 8-11, 2007.

[24] Nori, V. N., and Seitzman, J. M., "CH* Chemiluminescence Modeling for Combustion Diagnostics," submitted to *Proceedings of the Combustion Institute* **32**, 2008.
[25] CHEMKIN™, www.ReactionDesign.com
[26] Kee, R., Grcar, J., Smooke, M., and Miller, J., "A Fortran Program for Modeling Steady Laminar One-Dimensional Premixed Flames," Sandia National Laboratories, Report No. SAND85-8240, 1985.
[27] Lutz, A. E., Kee, R.J., Grcar, J. F., and Rupley, F. M., "A Fortran Program for Computing Opposed Flow Diffusion Flames," Sandia National Laboratories, Report No. SAND96-8247, 1997.
[28] Smith, G. P., Golden, D. M., Frenklach, M., Moriarty, N. W., Eiteneer, B., Goldenberg, M., Bowman, C. T., Hanson, R. K., Song, S., Gardiner, W. C. Jr., Lissianski, V. V., and Qin, X., http://www.me.berkeley.edu/gri_mech/mech/
[29] Samaniego, J. M., Egolfopoulos, F. N., and Bowman, C. T., "CO_2* Chemiluminescence in Premixed Flames," *Combustion Science and Technology*, Vol. 109, 1995, pp. 183-203.
[30] Carl, S. A., Poppel, V. M., and Peeters, J., "Identification of the CH + O_2 → OH (A) + CO Reaction as the Source of OH(A-X) Chemiluminescence in C_2H_2/O/H/O_2 Atomic Flames and Determination of its Absolute Rate Constant over the Range T = 296 to 511 K," *Journal of Physical Chemistry A* **107**, 2003, pp. 11001-11007.
[31] Petersen E. L., and Kalitan, D. M., "Calibration and Chemical Kinetics Modeling of an OH Chemiluminescence Diagnostic," AIAA 2003-4493, 39th AIAA/ASME/SAE/ASEE Joint Propulsion Conference and Exhibit, 20-23 July 2003, Huntsville, Alabama.
[32] Hall, J. M., and Petersen, E. L., "An Optimized Kinetics Model for OH Chemiluminescence at High Temperatures and Atmospheric Pressures," *International Journal of Chemical Kinetics* **38** (12), 2006, pp. 714-724.
[33] Tamura, M., Berg, P. A., Harrington, J. E., Luque, J., Jeffries, J. B., Smith, G. P., and Crosley, D. R., "Collisional Quenching of CH(A), OH(A), and NO(A) in Low Pressure Hydrocarbon Flames," *Combust Flame* **144**, 1998, pp. 502-514.
[34] Hidaka, Y., Takahashi, S., Kawano, H., Suga, M., and Gardiner, W. C. Jr., "Shock-Tube Measurement of the Rate Constant for Excited OH ($A^2\Sigma^+$) Formation in the Hydrogen-Oxygen Reaction," *Journal of Physical Chemistry*, **86** (8), 1982, pp. 1429-1433.
[35] Elsamra, R., M., I., Vranckx, S., and Carl, S., A., "CH($A^2\Delta$) Formation in Hydrocarbon Combustion: The Temperature Dependence of the Rate Constant of the Reaction C_2H+O_2 -> CH($A^2\Delta$)+CO_2," *J. Phys. Chem*., **109,** 2005, pp. 10287-10293.
[36] Baulch, D. L., Drysdale, D. D., Duxbury, J., and Grant, S. J., *Evaluated Kinetic Data for High Temperature Reactions* **3**, Butterworths, London, 1976.
[37] Slack, M., and Grillo, A., "High-Temperature Rate Coefficient Measurements of CO+O Chemiluminescence," *Combustion and Flame* **59** (2), 1985, pp. 189-196.
[38] Ladommatos, N., Abdelhalim, S. M., Zhao, H. and Hu. Z., "The Effects of Carbon Dioxide in Exhaust Gas Recirculation on Diesel Engine Emissions," *Proceedings of the Institution of Mechanical Engineers, Part D-Journal of Automobile Engineering*, Vol. 212 (D1), 1998, pp. 25-42.
[39] Abd-Alla, G. H., "Using Exhuast Gas Recirculation in Internal Combustion Engines: A Review," *Energy Conversion and Management* **43**(8), 2002, pp. 1027-1042.
[40] Zheng, M., Reader, G. T., and Hawley, J. G., "Diesel Engine Exhaust Gas Recirculation - A Review on Advanced and Novel Concepts," *Energy Conversion and Management* **45** (6), 2004, pp. 883-900.